JOURNAL OF BACTERIOLOGY, Mar. 2011, p. 1385–1392 Vol. 193, No. 6
0021-9193/11/$12.00 doi:10.1128/JB.01473-10

Genetic Analysis of the Protein Shell of the Microcompartments Involved in Coenzyme B_{12}-Dependent 1,2-Propanediol Degradation by *Salmonella*▽†

Shouqiang Cheng,[1] Sharmistha Sinha,[1] Chenguang Fan,[1] Yu Liu,[2] and Thomas A. Bobik[1]*

Department of Biochemistry, Biophysics and Molecular Biology, Iowa State University, Ames, Iowa 50011,[1] and Department of Plant and Microbial Biology, University of California, Berkeley, Berkeley, California 94720[2]

Received 6 December 2010/Accepted 3 January 2011

Hundreds of bacterial species use microcompartments (MCPs) to optimize metabolic pathways that have toxic or volatile intermediates. MCPs consist of a protein shell encapsulating specific metabolic enzymes. In *Salmonella*, an MCP is used for 1,2-propanediol utilization (Pdu MCP). The shell of this MCP is composed of eight different types of polypeptides, but their specific functions are uncertain. Here, we individually deleted the eight genes encoding the shell proteins of the Pdu MCP. The effects of each mutation on 1,2-PD degradation and MCP structure were determined by electron microscopy and growth studies. Deletion of the *pduBB′*, *pduJ*, or *pduN* gene severely impaired MCP formation, and the observed defects were consistent with roles as facet, edge, or vertex protein, respectively. Metabolite measurements showed that *pduA*, *pduBB′*, *pduJ*, or *pduN* deletion mutants accumulated propionaldehyde to toxic levels during 1,2-PD catabolism, indicating that the integrity of the shell was disrupted. Deletion of the *pduK*, *pduT*, or *pduU* gene did not substantially affect MCP structure or propionaldehyde accumulation, suggesting they are nonessential to MCP formation. However, the *pduU* or *pduT* deletion mutants grew more slowly than the wild type on 1,2-PD at saturating B_{12}, indicating that they are needed for maximal activity of the 1,2-PD degradative enzymes encased within the MCP shell. Considering recent crystallography studies, this suggests that PduT and PduU may mediate the transport of enzyme substrates/cofactors across the MCP shell. Interestingly, a *pduK* deletion caused MCP aggregation, suggesting a role in the spatial organization of MCP within the cytoplasm or perhaps in segregation at cell division.

Many diverse bacteria use proteinaceous microcompartments (MCPs) as simple organelles for the optimization of metabolic pathways that have toxic or volatile intermediates (4, 11, 14, 61). Bacterial MCPs are polyhedral in shape and 100 to 150 nm in cross-section (about the size of a large virus) and consist of a protein shell that encapsulates metabolic enzymes. They are composed of 10,000 to 20,000 polypeptides of 10 to 20 types, and there is no evidence for lipid components. Based on sequence analysis, it is estimated that MCPs are produced by 20 to 25% of bacteria and function in seven or more different metabolic processes (2, 4, 14). Different types of MCPs have related protein shells but differ in their encapsulated enzymes. In the cases that have been studied, MCPs encase enzymes that catalyze sequential reactions with a toxic or volatile intermediate. The best-studied MCP is the carboxysome, which is used to enhance autotrophic CO_2 fixation by confining CO_2 in the immediate vicinity of ribulose bisphosphate carboxylase monooxygenase (11, 42). Other MCPs are used to confine toxic/volatile aldehydes formed during the catabolism of ethanolamine and 1,2-propanediol (1,2-PD) or have unknown functions (8, 24, 41, 46, 47, 54). The protein shell of MCPs is thought to act as a diffusion barrier that helps retain the volatile/toxic intermediate and channel it to downstream enzymes (19, 24, 41, 44).

The protein shells of bacterial MCPs are typically composed of 5 to 10 different proteins that have bacterial microcompartment (BMC) domains (60). Recent crystallography of BMC proteins from several organisms has provided insights into the structural basis of shell assembly and function (17, 26, 32, 33, 48, 55, 56). In crystals, single-BMC-domain proteins usually form flat hexamers that tile into molecular sheets proposed to form the facets of the shell (32). Shell proteins with two tandem BMC domains form hexagonal trimers suitably shaped to form mixed sheets with single-BMC-domain proteins, suggesting that MCP shells are a mosaic of different types of BMC domain proteins (26, 33, 48). Another BMC protein (EutS) is a bent hexamer that could form the edges of the shell (57). A striking feature of BMC domain proteins is that they have central pores thought to mediate the transport of enzyme cofactors, substrates, and products between the interior of the MCP and the cytoplasm of the cell (32). Different shell proteins have pores that differ in charge and size, suggesting substrate selectivity (17, 26, 32, 33, 48, 55, 56). Moreover, some BMC domain proteins appear to have gated pores, and in one instance a BMC domain protein has an iron-sulfur center that might be used to conduct electrons between the cell cytoplasm and the interior of the MCP (16, 39). Lastly, a BMC domain fused to a probable DNA-binding protein was reported (57), and one class of shell protein which lacks a recognizable BMC domain (CcmL type) forms pentamers proposed to form the vertices of the shell (55). Overall, structural studies suggest that the shells of diverse MCPs are built from several types of

* Corresponding author. Mailing address: Iowa State University, Department of Biochemistry, Biophysics and Molecular Biology, Ames, IA 50011. Phone: (515) 294-4165. Fax: (515) 294-0453. E-mail: bobik@iastate.edu.

† Supplemental material for this article may be found at http://jb.asm.org/.

▽ Published ahead of print on 14 January 2011.

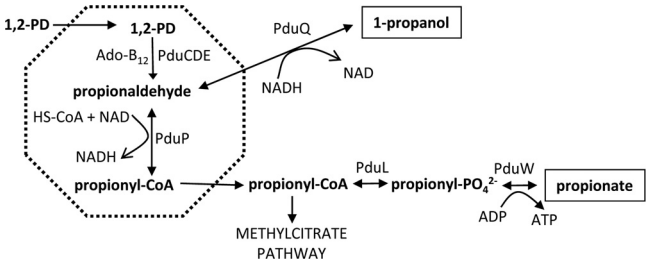

FIG. 1. Model for 1,2-propanediol degradation by *Salmonella*. The dashed line indicates the shell of the MCP, which is composed of eight different polypeptides (PduABB′JKNTU). The first two steps of 1,2-PD degradation occur in the lumen of the compartment and the remaining steps in the cytoplasm. The function of the Pdu MCP is to sequester the propionaldehyde produced by the first reaction of 1,2-PD degradation to minimize its toxicity. For the Pdu MCP to function, enzyme substrates, products, and cofactors must cross the shell and the MCP must segregate properly during cell division. Abbreviations: 1,2-PD, 1,2-propanediol; PduCDE, coenzyme B_{12}-dependent diol dehydratase; PduP, propionaldehyde dehydrogenase; PduL, phosphotransacylase; PduW, propionate kinase; PduQ, 1-propanol dehydrogenase.

functionally specialized shell proteins needed for assembly of the shell, metabolite transport, and other functions.

Our prior studies showed that an MCP is used for coenzyme B_{12}-dependent 1,2-PD utilization (Pdu MCP) by *Salmonella enterica* (4, 6, 7, 17, 23, 24, 34, 35, 50). 1,2-PD is a major product of the anaerobic degradation of the common plant sugars rhamnose and fucose, and this product is thought to be an important carbon and energy source in anoxic environments such as sediments, the depths of soils, and the large intestines of higher animals (38). Moreover, the capacity to degrade 1,2-PD is tentatively linked to pathogenesis in *Salmonella* and *Listeria* (9, 15, 25, 31). The first two steps of 1,2-PD degradation take place within the lumen of the Pdu MCP, where 1,2-PD is converted to propionaldehyde and then to propionyl-coenzyme A (CoA) by B_{12}-dependent diol dehydratase (PduCDE) and propionaldehyde dehydrogenase (PduP), respectively (Fig. 1) (23, 24, 34). Propionyl-CoA is thought to exit the MCP into the cytoplasm, where it is converted to propionate or enters central metabolism via the methylcitrate pathway (27, 38). The shell of the Pdu MCP is proposed to confine the propionaldehyde formed in the first step of 1,2-degradation in order to mitigate its toxicity as well as reduce DNA damage and limit diffusive loss through the cell membrane into the environment (6, 23, 24). The genes for 1,2-PD utilization (*pdu*) are found in a single contiguous cluster (*pocR*, *pduF*, *pduABB′ CDEGHJKLMNOPQSTUVWX*) (5–7, 12, 20, 21, 30, 34, 35, 45). Analyses of purified MCPs and labeling studies indicate that the Pdu MCP is composed of at least 17 polypeptides, all of which are encoded by the *pdu* operon (the PduABB′CDEGH JKNOPSTUV gene) (13, 23, 40). The shell of the Pdu MCP is thought to include eight different polypeptides (PduABB′JK NTU) (23). PduABB′JKTU have a BMC domain(s), and PduN is homologous to a pentamer that forms the vertices of the carboxysome shell (6). Prior studies with *Salmonella* showed that PduA is a component of the shell (24) and that *pduAB* or *pduJK* double deletion mutants were defective in MCP formation (24, 50). In addition, these double mutants where shown to accumulate propionaldehyde to toxic levels, resulting in a 20-hour period of growth arrest and increased DNA damage, indicating that a primary function of the Pdu MCP is to mitigate propionaldehyde toxicity (24, 50). In more-recent studies, the *Citrobacter pdu* operon was expressed in *Escherichia coli* and shown to mediate the formation of MCPs (39). Further studies in this system showed that the *pduA* or *pduBB′* genes were required for MCP formation (39). Very recently, the *Citrobacter* PduABB′JKN proteins were produced in recombinant *E. coli* and shown to be necessary and sufficient for formation of what appeared to be empty MCP shells, suggesting that they are structural proteins of the MCP shell (40). Thus, prior studies suggest that the PduABB′JKNTU proteins are shell components. However, their specific roles are uncertain, and the effects of deleting these genes singly (with the exception of *pduA* and *pduBB′*) on MCP structure and 1,2-PD degradation have not been reported previously. Therefore, to better understand the specific functional and structural roles of the Pdu MCP shell proteins, we constructed in-frame deletion mutants of each *Salmonella pdu* shell gene individually (*pduA*, *pduBB′*, *pduJ*, *pduK*, *pduN*, *pduT*, and *pduU*) and determined their effects on MCP structure and 1,2-PD catabolism using electron microcopy, growth studies, and metabolite measurements.

MATERIALS AND METHODS

Bacterial strains, media, and growth conditions. The bacterial strains used in this study are listed in Table 1. The rich medium used was Luria-Bertani/Lennox (LB) medium (Difco, Detroit, MI) (36). The minimal medium used was no-carbon-E (NCE) medium (3, 58).

Chemicals and reagents. Antibiotics were from Sigma Chemical Company (St. Louis, MO). Isopropyl-β-D-thiogalactopyranoside (IPTG) was from Diagnostic Chemicals Limited (Charlotteville PEI, Canada). Restriction enzymes and T4 DNA ligase were from New England BioLabs (Beverly, MA). Other chemicals were from Fisher Scientific (Pittsburgh, PA).

General molecular methods. Agarose gel electrophoresis, plasmid purification, PCR, restriction digests, ligation reactions, and electroporation were carried out using standard protocols as previously described (35, 49). Plasmid DNA was

TABLE 1. Bacterial strains used in this study

Strain[a]	Genotype	Source or reference
BE464	Δ*pduA687*::*frt*	This study
BE213	Δ*pduBB′675*	This study
BE184	Δ*pduJ654*	This study
BE770	Δ*pduK680*	This study
BE772	Δ*pduN681*::*frt*	This study
BE885	Δ*pduT682*::*frt*	This study
BE901	Δ*pduU683*::*frt*	This study
BE287	/pLAC22-no insert	59
TA1464	Δ*pduA687*::*frt*/pLAC22-*pduA*	This study
TA1409	Δ*pduBB′675*/pLAC22-*pduBB′*	This study
TA1411	Δ*pduBB′675*/pLAC22-no insert	This study
TA1412	Δ*pduJ654*/pLAC22-*pduJ*	This study
TA1414	Δ*pduJ654*/pLAC22-no insert	This study
BE777	Δ*pduK680*::*frt*/pLAC22-no insert	This study
BE778	Δ*pduK680*::*frt*/pLAC22-*pduK*	This study
BE779	Δ*pduN681*::*frt*/pLAC22-*no insert*	This study
BE780	Δ*pduN681*::*frt*/pLAC22-*pduN*	This study
BE918	Δ*pduT682*::*frt*/pLAC22-*pduT*	This study
BE917	Δ*pduT682*::*frt*/pLAC22-no insert	This study
BE924	Δ*pduU683*::*frt*/pLAC22-*pduU*	This study
BE925	Δ*pduU683*::*frt*/pLAC22-no insert	This study

[a] All strains are derivatives of *Salmonella enterica* serovar Typhimurium LT2.

purified by the alkaline lysis procedure (49) or by using Qiagen products (Qiagen, Chatsworth, CA) according to the manufacturer's instructions. Following restriction digestion or PCR amplification, DNA was purified using Promega Wizard PCR Preps (Madison, WI) or Qiagen gel extraction kits. Restriction digests were carried out using standard protocols (49). For ligation of DNA fragments, T4 DNA ligase was used according to the manufacturer's directions. Electroporation was carried out as previously described (6).

P22 transduction. Transductional crosses were performed as previously described, using P22 HT105/1 *int-210*, a mutant phage that has high transducing ability (53). Transductants were tested for phage contamination and sensitivity by streaking on green plates against P22 H5.

Construction of clones for complementation studies. The coding sequences of *pduA*, *pduBB′*, *pduJ*, *pduK*, *pduN*, *pduT*, and *pduU* were cloned into pLAC22 via PCR with template pEM55 as previously described (6). Vector pLAC22 allows tight regulation of protein production by IPTG (59). The DNA sequences of all clones were verified.

Construction of *pdu* deletion mutants. Two PCR-based methods were used to construct *pdu* deletion mutants. In each case, deletions removed nearly the entire coding sequence but left predicted translation signals of all *pdu* genes intact. The *pduBB′* and *pduJ* deletions were made by the method of Miller and Mekalanos with modifications previously described (37). The *pduA*, *pduK*, *pduN*, *pduT*, and *pduU* deletions were made by linear transformation of PCR products with modifications as described previously (18, 24). For mutants made by linear transformation, the kanamycin resistance cassette was moved to wild-type *Salmonella* by P22 transduction and then removed using the *flp* recombinase as described previously (18). The DNA sequences of Del *pduA687* (BE464) and Del *pduK680* (BE770) were verified by direct sequencing of chromosomal DNA (1 μg/μl) purified using a Qiagen DNeasy tissue kit and using primers pduA-348FF (GCCCATCATACGGGAGATTCGAGC), pduA-114FR (CTG CCATAGCCGTCTCTCGTATAG), pduK448FF (ACACTCGCTGGTCGT GCATTA), and pduK431FR (AAGCGGCGACATATGGATAT). In addition, PCR was used to verify all deletions as described previously (18).

Growth studies. Growth rates were determined using a Synergy HT microplate reader (BioTek, Winooski, VT) as previously described (35). Doubling times were calculated from semilog plots, where doubling time was calculated as 0.693/(2.303)(slope of the linear region of the plot). For determination of propionaldehyde levels, 50-ml cultures were grown in 250-ml Erlenmeyer flasks at 37°C with shaking at 275 rpm in an Innova I2400 incubator shaker (New Brunswick Scientific) (24). These cultures were inoculated to an optical density at 600 nm (OD_{600}) 0.1 with an LB overnight culture that had been centrifuged and resuspended in NCE with 1 mM $MgSO_4$.

Propionaldehyde determination. Cultures were sampled at timed intervals. Cells were removed by centrifugation followed by filtration with 0.22-μm Millex-GV syringe filters (Millipore Corporation). Propionaldehyde was then determined by high-performance liquid chromatography (HPLC) and by the 3-methyl-2-benzothiazolinone hydrazone (MBTH) assay as described previously (50).

Electron microscopy. For electron microscopy, strains were grown in 125-ml Erlenmeyer flasks containing 10 ml of NCE minimal medium supplemented with 1 mM $MgSO_4$, 0.5% succinate, 0.4% 1,2-PD, and 50 μM ferric citrate. Cultures were inoculated to an OD_{600} of 0.1 with an LB overnight culture that had been centrifuged and resuspended in NCE medium with 100 μM $MgSO_4$. After the cultures reached optical densities between 1 and 1.2 at 600 nm, cells were harvested by centrifugation. Imbedding, sectioning, and electron microscopy were carried out as described previously (6, 24).

SDS-PAGE and Western blots. Protein concentration was determined using Bio-Rad (Hercules, CA) protein assay reagent, with bovine serum albumin (BSA) as a standard. SDS-PAGE was performed using Bio-Rad 18% Tris-HCl ready gels. For Western blots, proteins were transferred from SDS-PADE gels to nitrocellulose membranes and detected by primary antibody from rabbit and goat anti-rabbit immunoglobulin conjugated to alkaline phosphatase as a secondary antibody (Bio-Rad). Chromogenic developing agents were used in accordance with the manufacturer's instructions (Bio-Rad).

DNA sequencing and analysis. DNA sequencing was carried out at the Iowa State University DNA Facility using Applied Biosystems, Inc., automated sequencing equipment. The template for DNA sequencing was plasmid DNA purified using Qiagen 100 tips or Qiagen miniprep kits. BLAST software was used for sequence similarity searching (1).

RESULTS

Electron microscopy of MCP shell mutants. Our prior studies indicated that the *pduA*, *pduB*, *pduB′*, *pduJ*, *pduK*, *pduN*, *pduT*, and *pduU* genes of *Salmonella* encode shell proteins of the Pdu MCP (23, 24, 50); however, the effects of deleting individual *Salmonella* shell protein genes on MCP structure have not been reported. Previously, a *Salmonella pduA* deletion mutant was investigated by our laboratory, but we later found that this mutant was constructed based on erroneous DNA sequence data and deleted both the *pduA* gene and the start of the *pduB* gene (24). Here, a new *pduA* deletion mutant was constructed based on a corrected DNA sequence, and electron microscopy was used to examine the effects of the *pduA*, *pduBB′*, *pduJ*, *pduK*, *pduN*, *pduT*, or *pduU* deletion mutations on the structure of the Pdu MCP of *Salmonella*. In all cases, several sections and hundreds of cells were examined from cultures grown on at least 2 different days. Representative images are presented in Fig. 2 and Fig. S2 to S9 in the supplemental material. Results showed that a strain with a *pduA* deletion formed MCPs that were somewhat enlarged compared to the wild type but generally similar in appearance (Fig. 2). For both wild-type *Salmonella* and the *pduA* deletion mutant, 40 MCPs were measured (80 total) in thin sections. Each MCP was measured twice, first on the longest axis and then 90 degrees to the first measurement, using ImageJ software (43) or manual measurements. The average of these two measurements was taken to indicate the cross-sectional length of the MCP. The mean cross-sectional length of wild-type MCPs ± 1 standard deviation was 123 ± 30 nm, compared to 155 ± 48 nm for MCPs from the *pduA* deletion mutant. We also plotted the size distribution of MCPs from wild type and the *pduA* mutant (Fig. S1). Compared to the wild type, the *pduA* mutant formed about 9-fold more MCPs that measured ≥180 nm. Thus, the *pduA* deletion mutant formed enlarged MCPs. This is in contrast to prior studies with the incorrect *pduA* mutant mentioned above (actually a *pduAB* double mutant), which did not form MCPs at all (24).

pduB and *pduB′* are overlapping genes (23, 39) and hence were deleted together. In a *pduBB′* deletion mutant, MCP formation was eliminated. No MCPs were observed in several hundred cells examined, and a single polar body was seen in about 20% of the cells (Fig. 2; see also Fig. S2 to S4 in the supplemental material). In addition, <1% contained unusual structures other than the polar bodies. Given their low numbers, these structures were most likely electron microscopy artifacts. In contrast, no polar bodies were observed in wild-type *Salmonella*, MCPs were present in >90% of cells, and unusual protein structures were seen in <1% of cells. Thus, the electron microscopy indicates that the *pduBB′* deletion mutant was unable to from MCPs.

In a strain with a *pduJ* deletion, highly elongated structures were observed in 22% of cells (Fig. 2). Further, ~20% of the examined cells contained amorphous inclusion bodies similar in appearance to those seen for the *pduBB′* deletion mutant. Most cells (57%) lacked MCPs or other unusual structures. Fewer than 1% of cells contained unusual protein structures of uncertain origin. This is in stark contrast to what was found for the wild type, where ~90% of cells contained normal-appearing MCPs. Thus, a *pduJ* deletion either prevents MCP formation or leads to the formation of elongated structures. This tentatively suggests that assembly might arrest at two different steps in a *pduJ* mutants, raising the possibility of more than one assembly pathway.

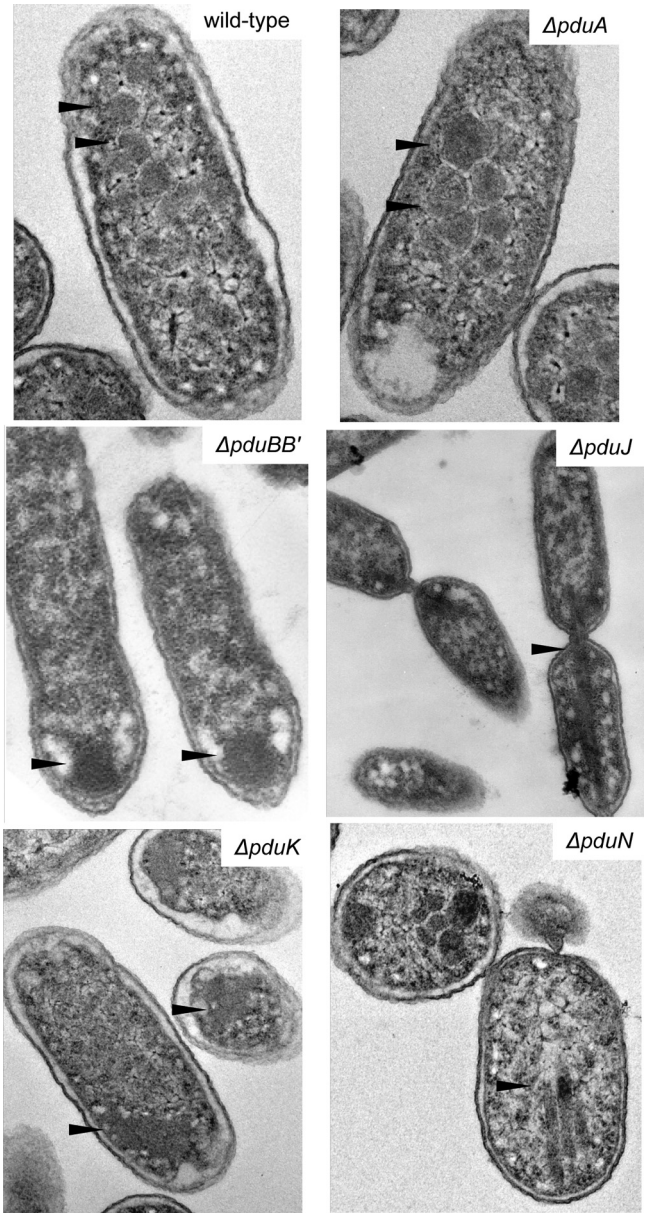

FIG. 2. Electron microscopy of wild-type *Salmonella* and selected deletion mutants. The bar is 200 nm. For more images, see Fig. S2 to S9 in the supplemental material.

A *pduK* deletion resulted in the formation of what appeared to be aggregates of MCPs (Fig. 2; see also Fig. S5 to S8 in the supplemental material) in ~52% of the cells examined. About 1% of cells contained unusual structures of uncertain origin. In ~47% of the cells examined, neither normal nor aggregated MCPs were detected. In contrast, no aggregates similar in appearance to those formed by the *pduK* deletion mutant were observed in wild-type cells, and ~90% of cells contained normal-appearing MCPs. The aggregates formed in *pduK* mutants differed from the polar bodies found in *pduBB′* mutants in that they appeared to be composed of MCPs delineated by shells, whereas the perimeters of the polar bodies were amorphous and lacked any observable indication of a shell. Moreover, growth studies and metabolite measurements indicated that the MCP aggregates formed in a *pduK* mutant function normally, supporting an intact shell (see below). Thus, we infer that a *pduK* deletion primarily results in the formation of aggregates of normally functioning MCPs.

A *pduN* mutant formed MCPs with a variety of morphologies, including elongated, enlarged, and aggregated MCPs and some with rounded cross-sections (Fig. 2; see also Fig. S9 in the supplemental material). The majority (~90%) of cells observed contained MCPs with unusual shapes. Based on visual appearance (size, shape, and staining density), we judge that few to none of the MCPs were of normal appearance. The variety of MCP sizes and shapes seen in a *pduN* deletion mutant is not easily described by size measurements; we therefore refer the reader to Fig. 2 and Fig. S9.

We also examined the effects of a *pduT* or a *pduU* deletion on MCP structure. These mutations had no obvious effects on MCP formation, based on electron microscopy observations (not shown). For the *pduU* and *pduT* mutants, ~90% of cells contained normal-appearing MCPs. By visual inspection, the size, shape, and staining density of MCPs from these mutants were similar to those of the wild type. The cross-sectional sizes of MCPs formed by *pduT* and *pduU* deletion mutants were determined as described above. The mean values ± 1 standard deviation were 121 ± 20 nm for the Δ*pduT* mutant and 113 ± 23 nm for the Δ*pduU* mutant compared to the value for the wild type, which was 123 ± 30 nm. In addition, the size distributions of MCPs found in the wild type and in *pduT* and *pduU* mutants were similar (see Fig. S1 in the supplemental material). Thus, *pduT* and *pduU* mutants form normal-appearing MCPs.

PduN is a component of the *Salmonella* Pdu MCP. PduN is homologous to CcmL and CsoS4A, which are non-BMC, pentameric proteins proposed to form the vertices of the carboxysomes (55). However, in prior studies, PduN was not identified as a component of purified *Salmonella* Pdu MCPs (23). This may have been due to low abundance. CsoS4A was not initially detected in purified carboxysomes (although it was detected in later studies by Western blot analysis), and individual icosahedra have only 12 vertex proteins among the hundreds of hexamers needed to form the triangular facets that comprise the bulk of the shell (10, 55). In addition, green fluorescent protein (GFP)-labeled PduN was shown to associate with what appear to be empty MCP shells when the PduABB′JKN proteins from *Citrobacter* are expressed from a plasmid in *E. coli* (40). Thus, PduN is thought to be a low-abundance component of the Pdu MCP. To directly test whether PduN is a component of intact *Salmonella* Pdu MCPs, Western blot anslyses were performed (see Fig. S10 in the supplemental material). A band near 12 kDa was detected in MCPs purified from wild-type *S. enterica*, while no PduN band was detected in MCPs purified from the *pduN* deletion mutant. Furthermore, when similar amounts of protein were analyzed, Western blot analysis readily detected PduN in purified MCPs but not in crude cell extracts (Fig. S10). This indicated that purified MCPs were enriched in PduN, strongly indicating that PduN protein is a component of intact Pdu MCPs from *Salmonella*.

Growth of MCP shell mutants on 1,2-PD with saturating or limiting B_{12}. Prior studies showed that strains of *Salmonella* having a *pduAB* or *pduJK* double deletion were unable to form

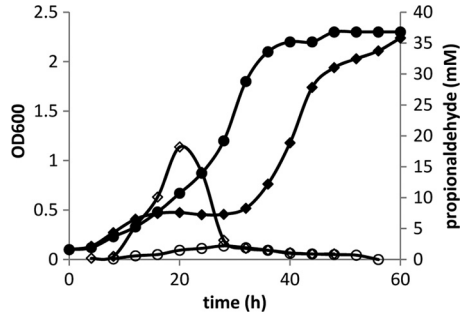

FIG. 3. Growth and propionaldehyde production by wild-type *Salmonella* and a *pduBB′* deletion mutant during growth on 1,2-PD minimal medium at saturating B_{12} (150 nm). Wild type: growth (closed circles) and propionaldehyde production (open circles). *pduBB′* deletion mutant: growth (closed diamonds) and propionaldehyde production (open diamonds). The *pduBB′* deletion mutant underwent a period of growth arrest between 12 and 32 h that corresponded with a spike in propionaldehyde levels. Generally similar results were obtained with *pduA*, *pduBB′ pduJ*, and *pduN* deletion mutants (see text). Cultures were grown in 250-ml flasks, and samples were removed at timed intervals to determine optical density and propionaldehyde levels in the culture medium.

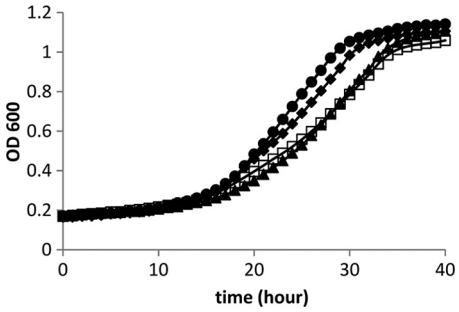

FIG. 4. Growth of *pduK*, *pduT*, and *pduU* deletion mutants on 1,2-propanediol with saturating B_{12} (150 nm). Wild-type *Salmonella* (closed circles) and Δ*pduK* (closed diamonds), Δ*pduT* (open squares), and Δ*pduU* (closed triangles) mutants. Growth curves were obtained with a Biotek Synergy microplate reader as described in Materials and Methods.

MCPs and accumulated propionaldehyde to levels that induced 20 to 30 h of growth arrest and increased DNA damage, supporting the idea that the Pdu MCP functions to minimize propionaldehyde toxicity (50). For this report, we conducted growth studies on strains with nonpolar deletions in *pduA*, *pduBB′*, *pduJ*, *pduK*, *pduN*, *pduT*, or *pduU* individually and on wild-type *Salmonella*. At saturating B_{12}, the wild type grew normally and accumulated propionaldehyde to about 2 mM (Fig. 3). Under similar growth conditions, two classes of mutants were found. For *pduA*, *pduBB′*, *pduJ*, and *pduN* deletion mutants, propionaldehyde accumulated to 12 to 20 mM and induced a period of growth arrest that lasted 15 to 20 h. The results obtained with a *pduBB′* deletion mutant are shown in Fig. 3. For this mutant, growth arrest lasted 20 h and propionaldehyde peaked at 18.2 mM. For *pduA*, *pduJ*, and *pduN* deletion mutants, the following values were obtained for growth arrest and maximum propionaldehyde level: for Δ*pduA*, 12 h and 12 mM; for Δ*pduJ*, 16 h and 14 mM; and for Δ*pduN*, 20 h and 16 mM. The growth rates for *pduA*, *pduBB′*, *pduJ*, and *pduN* deletion mutants were about the same as those for the wild type (1.2, 1.0, 1.2, and 0.93 times the wild-type rate, respectively) at saturating B_{12} (Table 2). In contrast, for *pduK*, *pduT*, and *pduU* deletion mutants, propionaldehyde levels stayed below 2 mM (similar to the wild-type level), and growth rates with 1,2-PD and saturating B_{12} were similar to the wild-type rate for the Δ*pduK* mutant (0.96 relative to the wild-type rate) and moderately impaired for the Δ*pduT* and Δ*pduU* mutants (0.67 and 0.66 times the wild-type rate, respectively) (Fig. 4 and Table 2).

Prior studies also showed that a *pduAB* double deletion mutant grew faster than the wild type during growth on 1,2-PD with limiting B_{12} (<50 nm) (24). This suggests that the shell of the Pdu MCP acts as a barrier to B_{12}, which is a required cofactor for the diol dehydratase enzyme (PduCDE) encased within the MCP (24). Here, we found that strains with mutations in *pduA*, *pduBB′*, *pduJ*, or *pduN* also grew substantially faster than wild-type *S. enterica* at 20 nm B_{12} (2.2, 3.9, 2.4, or 4.1 times the wild-type rate, respectively) (Fig. 5A and Table 2). In contrast, however, strains with *pduK*, *pduT*, or *pduU* mutations grew at about the same rate as wild-type at limiting B_{12} (1.02, 0.94, or 1.02 times the wild-type rate, respectively) (Fig. 5B and Table 2). The *pduU* deletion mutant was somewhat unusual in that it showed an increased lag time compared to the wild type and grew to a higher cell density. For the above-mentioned studies, growth rates (Table 2) were determined with a microplate reader using 6 replicates for each strain. Propionaldehyde was determined from cultures grown in shake flasks. This was done to provide sufficient amounts of sample for metabolite analyses and for consistency with prior studies (24) since culture conditions could affect the production of propionaldehyde and other metabolites. The observed growth phenotypes on 1,2-PD medium with saturating or limiting B_{12} indicate that PduA, PduBB′, PduJ, and PduN are

TABLE 2. MCP phenotypes of *pdu* deletion mutants

Relevant genotype (strain)	MCP formation	Growth arrest	Doubling time with B_{12} (h)		Growth lag on 1,2-PD minimal medium (h)
			Limiting	Saturating	
Wild-type *S. enterica* LT2	Normal	No	16.9 ± 0.83	5.4 ± 0.11	17.4 ± 0.3
Δ*pduA* (BE464)	Enlarged	Yes	7.8 ± 0.44	4.5 ± 0.25	17.5 ± 0.3
Δ*pduBB′* (BE213)	Absent, with polar body present	Yes	4.3 ± 0.10	5.2 ± 0.07	13.4 ± 0.1
Δ*pduJ* (BE184)	Elongated or amorphous	Yes	7.1 ± 0.52	4.5 ± 0.11	16.1 ± 0.5
Δ*pduK* (BE770)	Aggregated	No	16.6 ± 0.37	5.6 ± 0.17	17.6 ± 0.1
Δ*pduN* (*BE772*)	Elongated and varied shapes	Yes	4.1 ± 0.41	5.8 ± 0.16	15.9 ± 0.3
Δ*pduT* (BE885)	Normal	No	18.0 ± 1.13	8.1 ± 0.15	18.2 ± 0.3
Δ*pduU* (BE901)	Normal	No	16.5 ± 0.60	8.2 ± 0.28	20.0 ± 0.2

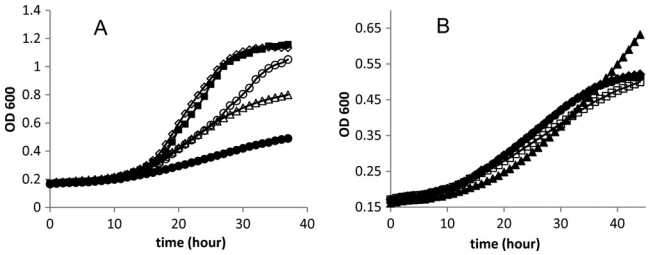

FIG. 5. Growth of *Salmonella pdu* shell gene deletion mutants on 1,2-propanediol with limiting B_{12} (20 nM). (A) Wild-type (closed circles) and Δ*pduA* (open triangles), Δ*pduBB′* (open diamonds), Δ*pduJ* (open circles), and Δ*pduN* (closed squares) mutants. (B) Wild-type *Salmonella* (closed circles) and Δ*pduK* (closed diamonds), Δ*pduU* (closed triangles), and Δ*pduT* (open squares) mutants. The growth curves for the wild type and the Δ*pduK* mutant are difficult to distinguish because they largely overlap. The growth medium was NCE minimal medium with 0.4% 1,2-PD and 20 nM vitamin B_{12}.

required for the structural integrity of the MCP shell but that PduK, PduT, and PduU are not and hence may have specialized functional roles.

Complementation studies. Studies were performed to determine whether the growth phenotypes of the *pduA*, *pduBB′*, *pduJ*, *pduK*, *pduN*, *pduT*, or *pduU* mutants could be complemented by the corresponding clone expressed from a plasmid. For the *pduA*, *pduBB′*, *pduJ*, and *pduN* deletion mutants, limiting B_{12} was used, and for the *pduK*, *pduT*, and *pduU* deletion mutants, saturating B_{12} was used. The vector used for complementation was pLAC22, which allows tight regulation of gene expression by IPTG (59). For the *pduBB′*, *pduJ*, *pduK*, *pduN*, *pduT*, and *pduU* deletion mutants, complementation was observed between 0.01 and 0.5 mM IPTG, indicating that the observed growth phenotypes were the result of the mutation under investigation and not due to polarity or an unknown mutation. In the case of the *pduA* deletion mutant, partial complementation was observed when the inoculum was grown in the presence of 1 mM IPTG to preinduce expression of *pduA*. No complementation was observed without preinduction (in contrast to what was found for the other deletion mutants tested). Three different *pduA* deletion mutants were constructed by linear transformation of PCR products, which is designed to generate nonpolar mutations (18, 37), and all three showed partial complementation. The DNA sequence of the *pduA* clone used for complementation and the *pduA* deletion present in BE464 were determined, and both were as expected. It is also clear that all three *pduA* deletion mutants were nonpolar, since each mutant grew well on 1,2-PD, which requires expression of multiple genes downstream of *pduA*. It seems most likely to us that the lack of full complementation was due to difficulty in establishing the precise gene dosage. Therefore, despite the lack of full complementation, it is likely the phenotypes observed for the *pduA* deletion mutant resulting from the *pduA* deletion.

DISCUSSION

In this study, we constructed precise deletion mutants of *pduA*, *pduBB′*, *pduJ*, *pduK*, *pduN*, *pduT*, and *pduU* individually and examined their phenotypes using electron microscopy, growth tests, and propionaldehyde measurements. The results showed that *pduA*, *pduBB′*, *pduJ*, and *pduN* were essential for MCP formation and mitigation of propionaldehyde toxicity. In addition, interpretation of the electron microscopy in terms of carboxysome structure (which is better understood) provides some additional insights. The carboxysome is icosahedral, with 20 triangular facets composed of hexagonal BMC domain proteins (28, 29, 52, 55). The triangular facets are thought to be joined by edge proteins (bent hexamers) and vertex proteins that impart the curvature needed to form a closed structure (55, 57). In this report, we showed that *pduJ* or *pduN* deletion mutants formed highly elongated MCPs, suggesting that these mutants are impaired for the formation of closed structures (Fig. 2). Given that PduJ comprises a substantial part of the total MCP protein (11%), PduJ is a good candidate for an edge protein that joins facets at the proper angle needed for closure. PduN is homologous to CcmL and CsoS4A, which are pentameric proteins proposed to form the vertices of the carboxysomes (55). Thus, results suggest that PduN is a vertex protein. However, EutN (which is also related to PduN in sequence) forms hexamers in crystals (22), and recent studies with *Halothiobacillus* have shown that strains carrying deletions of *csoS4*-A and *csoS4*-B form a minority of aberrant structures, suggesting that curvature also can be achieved without the presence of the CsoS4A and CsoS4B proteins (10). Thus, some unanswered questions remain regarding the role of PduN and the mechanism by which curvature is imparted to MCPs. We also examined a *pduBB′* deletion mutant which eliminates two overlapping genes. The *pduBB′* deletion prevented MCP formation and resulted in the formation of large amorphous inclusion bodies presumably composed of misassembled MCP proteins. Prior studies showed that the PduB and PduB′ proteins comprise nearly one-quarter of the total MCP protein, 12.8% and 12.1%, respectively (23). These findings are consistent with a role for PduBB′ as the major proteins that make up the facets of the shell interacting with both edge and vertex proteins and probably lumen enzymes as well. Accordingly, loss of PduBB′ resulted in the complete disassembly of the Pdu MCP. A *pduA* deletion mutant was also examined, and the results showed that it formed MCPs that were enlarged compared to those of the wild type but generally similar in appearance (Fig. 2). This is in contrast to the results reported for *Citrobacter*, where absence of *pduA* prevented MCP formation (39). It was somewhat surprising that deletion of *pduA* (which comprises about 7.5% of total MCP protein) (23, 24) had a relatively modest effect on MCP structure. This suggests that although PduA is a major component and essential for the mitigation of propionaldehyde toxicity, this protein may have a somewhat minor role in MCP assembly.

The phenotypes of *pduT* and *pduU* deletion mutants were also examined. The results indicated that these genes were nonessential for MCP formation and function (mitigation of propionaldehyde toxicity). In addition, prior studies showed that PduT and PduU are minor components of the Pdu MCP (23). Hence, studies suggest that PduT and PduU have specialized functional roles. These could include transport of enzyme substrates, products, cofactors, or electrons across the shell or the repair of Fe-S centers in lumen enzymes. These ideas are supported by the fact that crystal structures show that different shell proteins have Fe-S centers as well as pores that

differ in size and charge, suggesting that these proteins might selectively transport particular metabolites (16, 17, 26, 32, 33, 48, 55, 56). In addition, growth studies showed that *pduT* and *pduU* deletion mutants grew at about 67% of the rate of wild-type *Salmonella* at saturating B_{12} but at a rate similar to that of the wild type at limiting B_{12}. This suggests that PduT and PduU are needed to support maximal catalytic activity of the Pdu MCP for 1,2-PD degradation. This is consistent with the idea that PduT and PduU are used to improve the catalytic efficiency of the Pdu MCP perhaps by facilitating the movement of specific enzyme substrates, cofactors, or products across the MCP shell or by facilitating redox reactions. Prior structural studies showed that PduU has a circularly permuted BMC domain with a pore that is capped by a beta barrel that may serve as a gate during metabolite transport (17). Previous studies of PduT found that it has an iron-sulfur center located at its central pore, which might support electron transfer, redox regulation, or Fe-S repair (16, 39).

Lastly, we also investigated a *pduK* deletion mutant, with some unexpected results. The *pduK* deletion had no significant effect on propionaldehyde toxicity or on growth of *Salmonella* on 1,2-PD (Table 2). However, it did cause the MCPs to aggregate into clusters (Fig. 2; see also Fig. S5 to S8 in the supplemental material). Aggregation, with no apparent functional defect, suggests that the PduK protein may be important for spatial organization of the MCP within the cell or might have a role in segregation at cell division. Recent studies indicate that carboxysome spacing and segregation require ParA and MreB (51), but the manner in which these proteins interact with the carboxysome is unknown. In the case of the Pdu MCP, a tentative possibility is that PduK interacts with the cytoskeletal proteins such as ParA to promote proper spacing and segregation during division.

ACKNOWLEDGMENTS

This work was supported by grants MCB0956451 from the National Science Foundation and AI081146 from the National Institutes of Health.

We thank the ISU DNA Sequencing and Synthesis Facility for assistance with DNA analyses and the ISU Microscopy and Nanoimaging Facility of the Office of Biotechnology for help with the electron microscopy.

REFERENCES

1. **Altschul, S. F., et al.** 1997. Gapped BLAST and PSI-BLAST: a new generation of protein database search programs. Nucleic Acids Res. **25:**3389–3402.
2. **Beeby, M., T. A. Bobik, and T. O. Yeates.** 2009. Exploiting genomic patterns to discover new supramolecular protein assemblies. Protein Sci. **18:**69–79.
3. **Berkowitz, D., J. M. Hushon, H. J. Whitfield, Jr., J. Roth, and B. N. Ames.** 1968. Procedure for identifying nonsense mutations. J. Bacteriol. **96:**215–220.
4. **Bobik, T. A.** 2006. Polyhedral organelles compartmenting bacterial metabolic processes. Appl. Microbiol. Biotechnol. **70:**517–525.
5. **Bobik, T. A., M. E. Ailion, and J. R. Roth.** 1992. A single regulatory gene integrates control of vitamin B_{12} synthesis and propanediol degradation. J. Bacteriol. **174:**2253–2266.
6. **Bobik, T. A., G. D. Havemann, R. J. Busch, D. S. Williams, and H. C. Aldrich.** 1999. The propanediol utilization (*pdu*) operon of *Salmonella enterica* serovar Typhimurium LT2 includes genes necessary for formation of polyhedral organelles involved in coenzyme B_{12}-dependent 1,2-propanediol degradation. J. Bacteriol. **181:**5967–5975.
7. **Bobik, T. A., Y. Xu, R. M. Jeter, K. E. Otto, and J. R. Roth.** 1997. Propanediol utilization genes (*pdu*) of *Salmonella typhimurium*: three genes for the propanediol dehydratase. J. Bacteriol. **179:**6633–6639.
8. **Brinsmade, S. R., T. Paldon, and J. C. Escalante-Semerena.** 2005. Minimal functions and physiological conditions required for growth of *Salmonella enterica* on ethanolamine in the absence of the metabolosome. J. Bacteriol. **187:**8039–8046.
9. **Buchrieser, C., C. Rusniok, F. Kunst, P. Cossart, and P. Glaser.** 2003. Comparison of the genome sequences of *Listeria monocytogenes* and *Listeria innocua*: clues for evolution and pathogenicity. FEMS. Immunol. Med. Microbiol. **35:**207–213.
10. **Cai, F., et al.** 2009. The pentameric vertex proteins are necessary for the icosahedral carboxysome shell to function as a CO_2 leakage barrier. PLoS One **4:**e7521.
11. **Cannon, G. C., et al.** 2001. Microcompartments in prokaryotes: carboxysomes and related polyhedra. Appl. Environ. Microbiol. **67:**5351–5361.
12. **Chen, P., D. I. Andersson, and J. R. Roth.** 1994. The control region of the *pdu/cob* regulon in *Salmonella typhimurium*. J. Bacteriol. **176:**5474–5482.
13. **Cheng, S., and T. A. Bobik.** 2010. Characterization of the PduS cobalamin reductase of *Salmonella enterica* and its role in the Pdu microcompartment. J. Bacteriol. **192:**5071–5080.
14. **Cheng, S., Y. Liu, C. S. Crowley, T. O. Yeates, and T. A. Bobik.** 2008. Bacterial microcompartments: their properties and paradoxes. Bioessays **30:**1084–1095.
15. **Conner, C. P., D. M. Heithoff, S. M. Julio, R. L. Sinsheimer, and M. J. Mahan.** 1998. Differential patterns of acquired virulence genes distinguish *Salmonella* strains. Proc. Natl. Acad. Sci. U. S. A. **95:**4641–4645.
16. **Crowley, C. S., et al.** 2010. Structural insights into the mechanisms of transport across the *Salmonella enterica* Pdu microcompartment shell. J. Biol. Chem. **285:**37838–37846.
17. **Crowley, C. S., M. R. Sawaya, T. A. Bobik, and T. O. Yeates.** 2008. Structure of the PduU shell protein from the Pdu microcompartment of *Salmonella*. Structure **16:**1324–1332.
18. **Datsenko, K. A., and B. L. Wanner.** 2000. One-step inactivation of chromosomal genes in *Escherichia coli* K-12 using PCR products. Proc. Natl. Acad. Sci. U. S. A. **97:**6640–6645.
19. **Dou, Z., et al.** 2008. CO_2 fixation kinetics of *Halothiobacillus neapolitanus* mutant carboxysomes lacking carbonic anhydrase suggest the shell acts as a diffusional barrier for CO_2. J. Biol. Chem. **283:**10377–10384.
20. **Fan, C., and T. A. Bobik.** 2008. The PduX enzyme of *Salmonella* enterica is an L-threonine kinase used for coenzyme B_{12} synthesis. J. Biol. Chem. **283:**11322–11329.
21. **Fan, C., H. J. Fromm, and T. A. Bobik.** 2009. Kinetic and functional analysis of L-threonine kinase, the PduX enzyme of *Salmonella enterica*. J. Biol. Chem. **284:**20240–20248.
22. **Forouhar, F., et al.** 2007. Functional insights from structural genomics. J. Struct. Funct. Genomics **8:**37–44.
23. **Havemann, G. D., and T. A. Bobik.** 2003. Protein content of polyhedral organelles involved in coenzyme B_{12}-dependent degradation of 1,2-propanediol in *Salmonella enterica* serovar Typhimurium LT2. J. Bacteriol. **185:**5086–5095.
24. **Havemann, G. D., E. M. Sampson, and T. A. Bobik.** 2002. PduA is a shell protein of polyhedral organelles involved in coenzyme B_{12}-dependent degradation of 1,2-propanediol in *Salmonella enterica* serovar Typhimurium LT2. J. Bacteriol. **184:**1253–1262.
25. **Heithoff, D. M., et al.** 1999. Coordinate intracellular expression of *Salmonella* genes induced during infection. J. Bacteriol. **181:**799–807.
26. **Heldt, D., et al.** 2009. Structure of a trimeric bacterial microcompartment shell protein, EtuB, associated with ethanol utilisation in *Clostridium kluyveri*. Biochem. J. **423:**199–207.
27. **Horswill, A. R., and J. C. Escalante-Semerena.** 1999. *Salmonella typhimurium* LT2 catabolizes propionate via the 2-methylcitric acid cycle. J. Bacteriol. **181:**5615–5623.
28. **Iancu, C. V., et al.** 2007. The structure of isolated *Synechococcus* strain WH8102 carboxysomes as revealed by electron cryotomography. J. Mol. Biol. **372:**764–773.
29. **Iancu, C. V., et al.** 2010. Organization, structure, and assembly of a-carboxysomes determined by electron cryotomography of intact cells. J. Mol. Biol. **396:**105–117.
30. **Johnson, C. L. V. J., et al.** 2001. Functional genomic, biochemical, and genetic characterization of the *Salmonella pduO* gene, an ATP:cob(I)alamin adenosyltransferase gene. J. Bacteriol. **183:**1577–1584.
31. **Joseph, B., et al.** 2006. Identification of *Listeria monocytogenes* genes contributing to intracellular replication by expression profiling and mutant screening. J. Bacteriol. **188:**556–568.
32. **Kerfeld, C. A., et al.** 2005. Protein structures forming the shell of primitive bacterial organelles. Science **309:**936–938.
33. **Klein, M. G., et al.** 2009. Identification and structural analysis of a novel carboxysome shell protein with implications for metabolite transport. J. Mol. Biol. **392:**319–333.
34. **Leal, N. A., G. D. Havemann, and T. A. Bobik.** 2003. PduP is a coenzyme A-acylating propionaldehyde dehydrogenase associated with the polyhedral bodies involved in B_{12}-dependent 1,2-propanediol degradation by *Salmonella enterica* serovar Typhimurium LT2. Arch. Microbiol. **180:**353–361.
35. **Liu, Y., et al.** 2007. PduL is an evolutionarily distinct phosphotransacylase involved in B_{12}-dependent 1,2-propanediol degradation by *Salmonella enterica* serovar Typhimurium LT2. J. Bacteriol. **189:**1589–1596.
36. **Miller, J. H.** 1972. Experiments in molecular genetics. Cold Spring Harbor Laboratory, Cold Spring Harbor, NY.

37. **Miller, V. L., and J. J. Mekalanos.** 1988. A novel suicide vector and its use in construction of insertion mutations: osmoregulation of outer membrane proteins and virulence determinants in *Vibrio cholerae* requires *toxR*. J. Bacteriol. **170:**2575–2583.
38. **Obradors, N., J. Badia, L. Baldoma, and J. Aguilar.** 1988. Anaerobic metabolism of the L-rhamnose fermentation product 1,2-propanediol in *Salmonella typhimurium*. J. Bacteriol. **170:**2159–2162.
39. **Parsons, J. B., et al.** 2008. Biochemical and structural insights into bacterial organelle form and biogenesis. J. Biol. Chem. **283:**14366–14375.
40. **Parsons, J. B., et al.** 2010. Synthesis of empty bacterial microcompartments, directed organelle protein incorporation, and evidence of filament-associated organelle movement. Mol. Cell **38:**305–315.
41. **Penrod, J. T., and J. R. Roth.** 2006. Conserving a volatile metabolite: a role for carboxysome-like organelles in *Salmonella enterica*. J. Bacteriol. **188:** 2865–2874.
42. **Price, G. D., M. R. Badger, F. J. Woodger, and B. M. Long.** 2008. Advances in understanding the cyanobacterial CO_2-concentrating-mechanism (CCM): functional components, Ci transporters, diversity, genetic regulation and prospects for engineering into plants. J. Exp. Bot. **59:**1441–1461.
43. **Rasband, W.** 1997. ImageJ. U.S. National Institutes of Health, Bethesda, MD. http://rsb.info.nih.gov/ij/.
44. **Reinhold, L., R. Kosloff, and A. Kaplan.** 1991. A model for inorganic carbon fluxes and photosynthesis in cyanobacterial carboxysomes. Can. J. Bot. **69:** 984–988.
45. **Rondon, M. R., and J. Escalante-Semerena.** 1992. The *poc* locus is required for 1,2-propanediol-dependent transcription of the cobalamin biosynthetic (*cob*) and propanediol utilization (*pdu*) genes of *Salmonella typhimurium*. J. Bacteriol. **174:**2267–2272.
46. **Rondon, M. R., A. R. Horswill, and J. C. Escalante-Semerena.** 1995. DNA polymerase I function is required for the utilization of ethanolamine, 1,2-propanediol, and propionate by *Salmonella typhimurium* LT2. J. Bacteriol. **177:**7119–7124.
47. **Rondon, M. R., R. Kazmierczak, and J. C. Escalante-Semerena.** 1995. Glutathione is required for maximal transcription of the cobalamin biosynthetic and 1,2-propanediol utilization (*cob*/*pdu*) regulon and for the catabolism of ethanolamine, 1,2-propanediol, and propionate in *Salmonella typhimurium* LT2. J. Bacteriol. **177:**5434–5439.
48. **Sagermann, M., A. Ohtaki, and K. Nikolakakis.** 2009. Crystal structure of the EutL shell protein of the ethanolamine ammonia lyase microcompartment. Proc. Natl. Acad. Sci. U. S. A. **106:**8883–8887.
49. **Sambrook, J., E. F. Fritsch, and T. Maniatis.** 1989. Molecular cloning: a laboratory manual, 2nd ed. Cold Spring Harbor Laboratory, Cold Spring Harbor, NY.
50. **Sampson, E. M., and T. A. Bobik.** 2008. Microcompartments for B_{12}-dependent 1,2-propanediol degradation provide protection from DNA and cellular damage by a reactive metabolic intermediate. J. Bacteriol. **190:**2966–2971.
51. **Savage, D. F., B. Afonso, A. H. Chen, and P. A. Silver.** 2010. Spatially ordered dynamics of the bacterial carbon fixation machinery. Science **327:**1258–1261.
52. **Schmid, M. F., et al.** 2006. Structure of *Halothiobacillus neapolitanus* carboxysomes by cryo-electron tomography. J. Mol. Biol. **364:**526–535.
53. **Schmieger, H.** 1971. A method for detection of phage mutants with altered transducing ability. Mol. Gen. Genet. **110:**378–381.
54. **Stojiljkovic, I., A. J. Baeumler, and F. Heffron.** 1995. Ethanolamine utilization in *Salmonella typhimurium*: nucleotide sequence, protein expression, and mutational analysis of the *cchA cchB eutE eutJ eutG eutH* gene cluster. J. Bacteriol. **177:**1357–1366.
55. **Tanaka, S., et al.** 2008. Atomic-level models of the bacterial carboxysome shell. Science **319:**1083–1086.
56. **Tanaka, S., M. R. Sawaya, M. Phillips, and T. O. Yeates.** 2009. Insights from multiple structures of the shell proteins from the beta-carboxysome. Protein Sci. **18:**108–120.
57. **Tanaka, S., M. R. Sawaya, and T. O. Yeates.** 2010. Structure and mechanisms of a protein-based organelle in *Escherichia coli*. Science **327:**81–84.
58. **Vogel, H. J., and D. M. Bonner.** 1956. Acetylornithinase of *Escherichia coli*: partial purification and some properties. J. Biol. Chem. **218:**97–106.
59. **Warren, J. W., J. R. Walker, J. R. Roth, and E. Altman.** 2000. Construction and characterization of a highly regulable expression vector, pLAC11, and its multipurpose derivatives, pLAC22 and pLAC33. Plasmid **44:**131–151.
60. **Yeates, T. O., C. S. Crowley, and S. Tanaka.** 2010. Bacterial microcompartment organelles: protein shell structure and evolution. Annu. Rev. Biophys. **39:**185–205.
61. **Yeates, T. O., C. A. Kerfeld, S. Heinhorst, G. C. Cannon, and J. M. Shively.** 2008. Protein-based organelles in bacteria: carboxysomes and related microcompartments. Nat. Rev. Microbiol. **6:**681–691.